ADVANCED FUNCTIONAL MATERIALS

A Novel Route to Thermosensitive Polymeric Core–Shell Aggregates and Hollow Spheres in Aqueous Media**

By *Youwei Zhang*, *Ming Jiang*,* *Jiongxin Zhao*, *Xianwen Ren*, *Daoyong Chen*, and *Guangzhao Zhang*

Poly(ε-caprolactone)/poly(*N*-isopropylacrylamide) (PCL/PNIPAM) core–shell particles are obtained by localizing the polymerization of NIPAM and crosslinker methylene bisacrylamide around the surface of PCL nanoparticles. The resultant particles are converted to hollow PNIPAM spheres by simply degrading the PCL core with an enzyme. The hollow spheres are thermosensitive and display a reversible swelling and de-swelling at ~32 °C.

1. Introduction

Macromolecular assemblies on nanometer or sub-micrometer scales, with either core–shell morphology or cavity-containing structures, have attracted great interest in recent years due to their broad potential applications.[1–4] Much effort has been made to prepare hollow spheres because of their potential ability to encapsulate large-sized—and a large quantity of—guest molecules. Core–shell micelles[5–11] or vesicles[12–14] of block copolymers are the most commonly used precursors for producing hollow spheres. In addition, methods such as layer-by-layer deposition on colloidal particle templates[15–20] and emulsion polymerization[21–24] have been developed for this purpose. Furthermore, in order to enable the transport and delivery of guest molecules under particularly demanding conditions, "intelligent" micelles and hollow spheres, which are sensitive to temperature,[18,24–27] pH,[2,12,13,19,28–32] ions,[19,33] and ionic strength,[17,34] have also been reported. Among the polymer materials employed for such assemblies, poly(*N*-isopropylacrylamide) (PNIPAM) has been extensively studied owing to its thermosensitive phase transition at the lower critical solution temperature (LCST) around 32 °C.[35,36]

In a significant development of our long-term research on self-assembly following our "block-copolymer-free" strategies,[37–42] herein we report a novel route to thermosensitive core–shell aggregates and hollow spheres, as well as their environment-sensitive properties.

2. Results and Discussion

The following facts were taken into account when the synthetic route shown in Figure 1 was designed: The initiator, azodiisobutyronitrile (AIBN) is hydrophobic, whereas the monomer (NIPAM) is hydrophilic; PNIPAM becomes hydrophobic in aqueous media when the temperature is higher than 32 °C; and poly(ε-caprolactone) (PCL) is hydrophobic and biodegradable. In the procedure, a solution of PCL in dimethylformamide (DMF) containing AIBN was added dropwise into water, leading to PCL nanoparticles.[43] NIPAM and methylene bisacrylamide (MBA) as the crosslinker were then introduced to the PCL dispersion; polymerization was initiated by raising the temperature to 76 °C. The polymerization was expected to take place at the periphery of the PCL nanoparticles, since it is more favorable for the hydrophobic initiator to reside in the hydrophobic PCL particles, whereas the hydrophilic monomer and crosslinker reside mainly in the water. Once the crosslinked PNIPAM chains form, it was expected that they would collapse and adhere to the PCL particles as a result of their hydrophobicity at temperatures above 32 °C. The first PNIPAM layer formed would further trap the monomer and crosslinker from the water phase, so that the polymerization would continue and the shell grow. It is noteworthy that although both PCL and PNIPAM are hydrophobic in water at 76 °C, they construct stable core–shell particles. PNIPAM nanoparticles remain stable above their LCST, as has been reported and discussed in the literature,[44,45] because the polar groups of PNIPAM preferentially present on the outer surface of the particles. The subsequent degradation of the PCL cores by the enzyme lipolase results in hollow spheres made of PNIPAM networks, which are also called nanocages.[8]

Typically, when the concentration of the PCL/DMF solution, the feed weight ratio of the monomer to PCL, and the target crosslinking degree of the shell were 10 mg mL^{-1}, 5:1, and 10 mol-%, respectively, the conversion reached about 76 % after 4.0 h polymerization. Meanwhile, the weight ratio of the crosslinked PNIPAM around the PCL cores to that in water

[*] Prof. M. Jiang, Y. Zhang, X. Ren, Prof. D. Chen
Department of Macromolecular Science and the Key Laboratory of Molecular Engineering of Polymers
Fudan University
Shanghai, 200433 (P.R. China)
mjiang@fudan.edu.cn
Y. Zhang, Prof. J. Zhao
College of Material Science and Engineering
Donghua University
Shanghai, 200051 (P.R. China)
Prof. G. Zhang
Department of Chemical Physics
University of Science and Technology of China
Hefei, 230026 (P.R. China)

[**] The National Natural Science Foundation of China (NNSFC Nos. 50173006, 50333010) is acknowledged for supporting this research.

 DOI: 10.1002/adfm.200400378

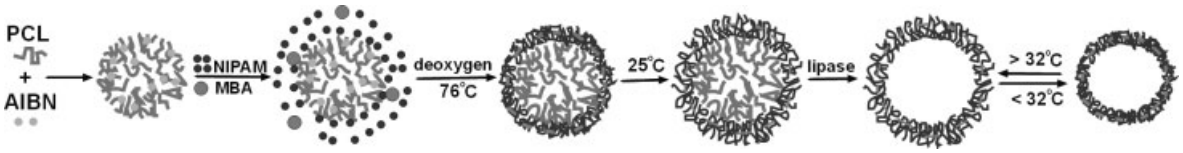

Figure 1. Schematic illustration of the preparation route to thermosensitive hollow spheres of crosslinked PNIPAM.

was found to be 3.5:1, which indicates that the polymerization did occur mainly around the PCL particles. A subsidiary experiment has indicated that the hydrophilic initiator potassium persulfate leads to a PNIPAM bulk gel instead of core–shell spheres under the same polymerization conditions.

Dynamic light scattering (DLS) was used to measure the average hydrodynamic diameter ($\langle D_h \rangle$) of a series of PCL/PNIPAM core–shell spheres as a function of temperature (Fig. 2). The samples are denoted as N*a*-*b*, where *a* represents the initial concentration of PCL in DMF (mg mL^{-1}) and *b* the weight ratio of the monomer plus crosslinker to PCL. Figure 2 clearly shows that the size of the spheres depends on the initial concentration of PCL when the monomer/PCL weight ratio is fixed. Over the whole temperature range, a higher initial PCL concentration gives rise to larger particles (compare curves 2, 3, and 4). Figure 2 also indicates that the thickness, and, accordingly, the overall size, of the particles increases with increasing relative monomer amount (compare curves 1, 2, and 5) when the initial PCL concentration or the core size is not changed. More importantly, the size of the core–shell particles shows a distinct dependence on temperature. The diameters and volumes of the particles increase approximately 1.6- and 4.1-fold, respectively, as the temperature decreases from 40 to 25 °C. It can also be seen that the thinnest shell almost does not display such a temperature dependence (curve 1) because the PNIPAM shell is too thin to make any detectable size change.

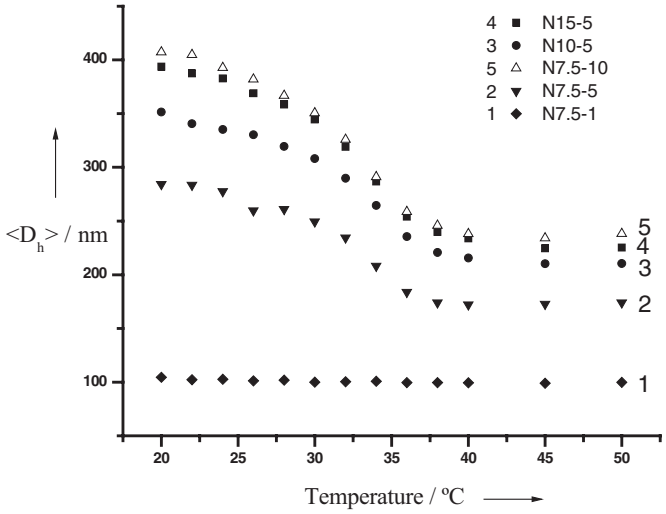

Figure 2. Average hydrodynamic diameters of various thermosensitive spheres obtained under different reaction conditions, as a function of temperature. For all the samples, the target degree of crosslinking (molar ratio of MBA/NIPAM) was 10 %. The measurements were performed at 90°.

The PCL/PNIPAM core–shell spheres can be converted to hollow spheres by removing the PCL cores by biodegradation. Lipolase, which selectively degrades aliphatic polyesters and fat[46,47] without affecting the amide links of the crosslinked PNIPAM, was chosen to hydrolyze the PCL core. DLS was used to trace the process of core degradation. Figure 3 shows the reaction-time dependence of the light scattering (I_s), which is proportional to the particle mass, and the average hydrodynamic diameter, for N10-5. The whole cavitation process can be divided into three stages. In the first stage, that is, from the beginning to about 180 min, I_s decreases rapidly while $\langle D_h \rangle$ increases slowly, implying that the swelling of the sphere shell is limited. In the second stage (180–400 min), I_s continues to decrease rapidly, accompanied by a fast increase in size, suggesting that the further removal of the core gradually enables the shell to swell freely. Finally, the sphere size and the scattering intensity become constant at about 1800 min, indicating that the core is completely degraded. After biodegradation, the sphere size has increased from 335 to about 374 nm. The resultant hollow spheres are denoted as H10-5.

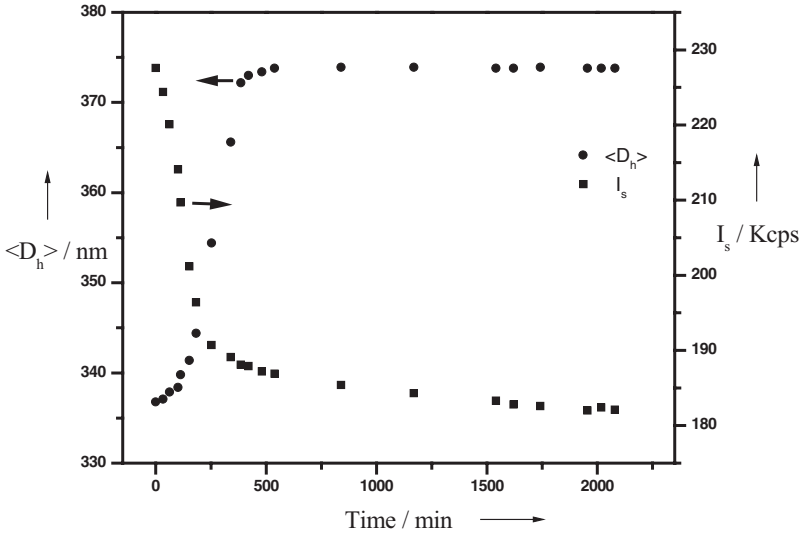

Figure 3. $\langle D_h \rangle$ and scattering intensity I_s of spheres N10-5 as a function of degradation time (40 μL lipolase solution was added to 2 mL N10-5 solution of 0.1 mg mL^{-1}). The measurements were performed at 90°.

ADVANCED FUNCTIONAL MATERIALS

A combination of DLS and static light scattering (SLS) measurements giving the ratio of the average gyration radius to the average hydrodynamic radius, $\langle R_g \rangle / \langle R_h \rangle$, which is sensitive to particle morphology, was conducted in order to explore the structural difference of the assemblies caused by degradation. As shown in Table 1, N10-5 has a $\langle R_g \rangle / \langle R_h \rangle$ of 0.75 at 20 °C, which is very close to the 0.77 of uniform spheres,[48,49] reflecting a small difference in the chain density between the PCL core and highly crosslinked shell of PNIPAM. After the core is degraded, a higher $\langle R_g \rangle / \langle R_h \rangle$ value of 0.86 was obtained for H10-5 at 20 °C, which is in accordance with the calculated value for thick-layer hollow spheres.[50] In addition, at 45 °C, the $\langle R_g \rangle / \langle R_h \rangle$ of H10-5 decreases to 0.75, which is close to the value of a uniform sphere. This indicates that above the LCST, the small cavity of H10-5 disappears or becomes much smaller due to the collapse of the PNIPAM network. However, the corresponding decrease in $\langle R_g \rangle / \langle R_h \rangle$ of the N10-5 spheres is much less pronounced, that is, from 0.75 to 0.73, which reflects a slight change in its morphology, since the PCL core is inert to a change in temperature.

Table 1. Light-scattering characterization data of the core–shell spheres N10-5 and the corresponding hollow spheres H10-5 [a].

Sample no.	Temp. [°C]	$\langle R_h \rangle$ [nm]	$\langle R_g \rangle$ [nm] [d]	$\langle R_g \rangle / \langle R_h \rangle$	PDI [e]
N10-5 [b]	20	201.1	151.4	0.753	0.04
N10-5 [b]	45	119.7	87.0	0.727	0.05
H10-5 [c]	20	217.0	186.8	0.861	0.01
H10-5 [c]	45	111.5	83.1	0.745	0.02

[a] An ALV/SP-125 LLS spectrometer was used, and the DLS measurements were performed at 15°. [b] The concentration of the N10-5 solution was 6.4×10^{-3} mg mL^{-1}. [c] The concentration of the H10-5 solution was 2.5×10^{-3} mg mL^{-1}. [d] SLS studies were performed at a low scattering-angle range, from 15 to 30° at 20 °C, and from 15 to 40° at 45 °C, the Guinier model was used for the SLS. [e] PDI: polydispersity index.

The data in Table 1 also show that both the core–shell spheres and the hollow spheres have narrow size distributions.

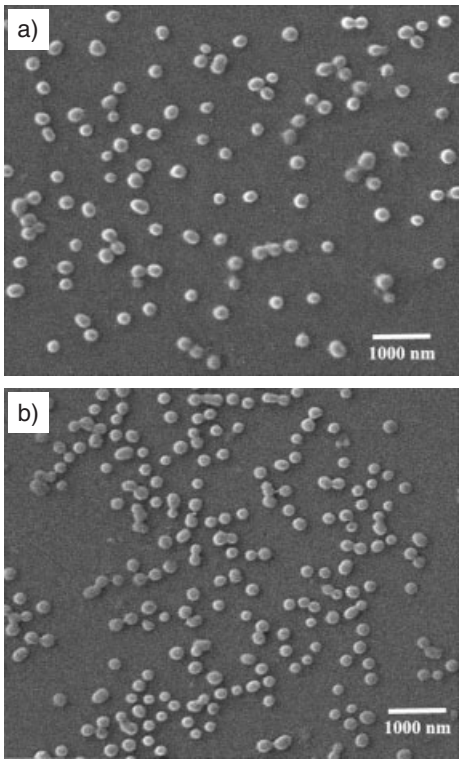

Figure 4. SEM images of a) N10-5 spheres and b) H10-5 hollow spheres.

Scanning electron microscopy (SEM) observations (Fig. 4) confirmed this conclusion. The typical hollow structure was not observed in the SEM image of the hollow spheres H10-5, due to their fairly thick shells. As reported before, we also did not see the hollow structure of crosslinked poly(vinyl alcohol), PVA, hollow spheres by SEM.[40]

The Fourier-transform infrared (FTIR) spectroscopy results (Fig. 5) provide additional evidence for the core removal: after the reaction of N10-5 with lipolase, the characteristic peak of

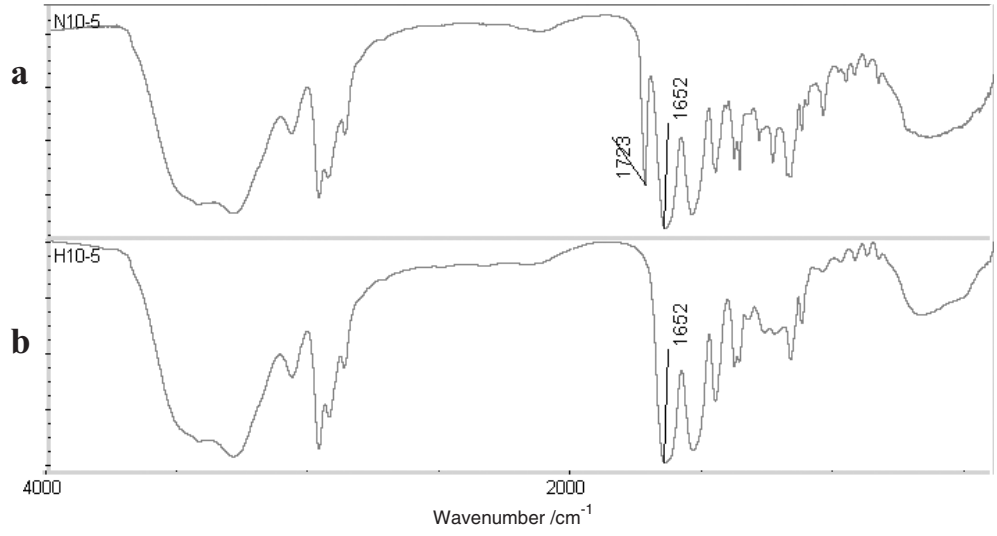

Figure 5. FTIR spectra of a) N10-5 spheres and b) H10-5 hollow spheres.

the ester group of PCL around 1724 cm^{-1} completely disappeared, while the peaks associated with the crosslinked PNIPAM remained.

Our major concern in this study is the thermally sensitive behavior of the hollow spheres. As shown in Figure 6, as the temperature increases from 20 °C to 45 °C, the diameter of the H10-5 hollow spheres decreases from 432 to 223 nm, corresponding to the "open" and "closed" states of the crosslinked PNIPAM shell, respectively. An abrupt change occurs between 27 and 35 °C, covering the range for the most pharmaceutical applications. Compared to its parent N10-5 core–shell spheres, the hollow spheres display an apparently larger dimensional change, that is, the PNIPAM nanocage can shrink and swell over a wider range of volume. Most important is the reversibility of the size dependence of the nanocage. The average hydrodynamic diameter of the nanocage in the heating process completely coincides with that in the cooling process. In other words, after a cycle of temperature increase and decrease, the sphere size returns to its starting value. No doubt, this perfect reversibility is a valuable property if the material is to be used repeatedly.

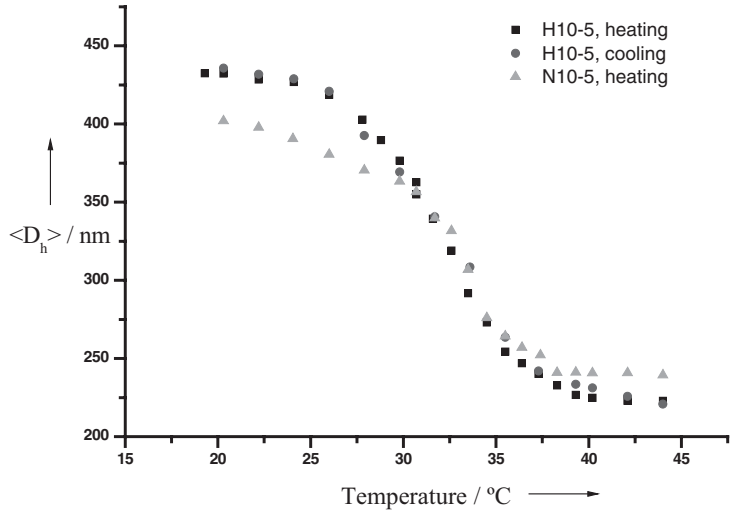

Figure 6. Average hydrodynamic diameters of the N10-5 core–shell spheres and H10-5 hollow spheres as a function of temperature. The measurements were performed at 15°.

The core–shell structure of the resultant assemblies was visualized using TEM. In Figure 7a, an image of N10-5 without staining, we can see clearly a dark circumference dividing two bright areas, that is, the core and the shell. We suppose that in the reaction solutions, NIPAM and MBA may diffuse into, and be absorbed in, the periphery of the PCL particles. The subsequent polymerization thus leads to a relatively high chain density in the core–shell interface. The apparent size shown in the microscope images is less than obtained from DLS measurements. This is obviously caused by constriction of the spheres due to drying in the process of sample preparation. Figure 7b displays the microimage of N10-5 after negative staining. This treatment strengthens the contrast between the shell and background, making the particle contour more distinct. In addition, the inner structure shown in Figure 7b is the same as that found without staining. The microstructure of H10-5 hollow spheres after negative staining is shown in Figure 7c. In contrast to Figure 7b, no internal structure is observed in Figure 7c. This is understandable as the degradation destroys the core as well as the interface, thus the dark circumference vanishes.

Further experiments proved that this procedure is a general method for producing core–shell particles and hollow spheres, provided that the monomer is hydrophilic and the corresponding polymer is hydrophobic under the polymerization conditions. 2-Hydroxypropyl methyacrylate (HPMA) and vinyl acetate (VAc) were successfully used for this purpose. These results will be reported elsewhere.

3. Conclusions

We have developed a new and convenient method for preparing thermally sensitive hollow spheres based on crosslinked PNIPAM. The polymerization of NIPAM and crosslinker MBA was initiated around the periphery of PCL particles, leading to core–shell aggregates. By degrading the PCL core with an enzyme, hollow spheres of PNIPAM were attained. The size and the shell thickness of the hollow spheres was easily adjusted. The PNIPAM nanocages exhibit reversible swelling and de-swelling

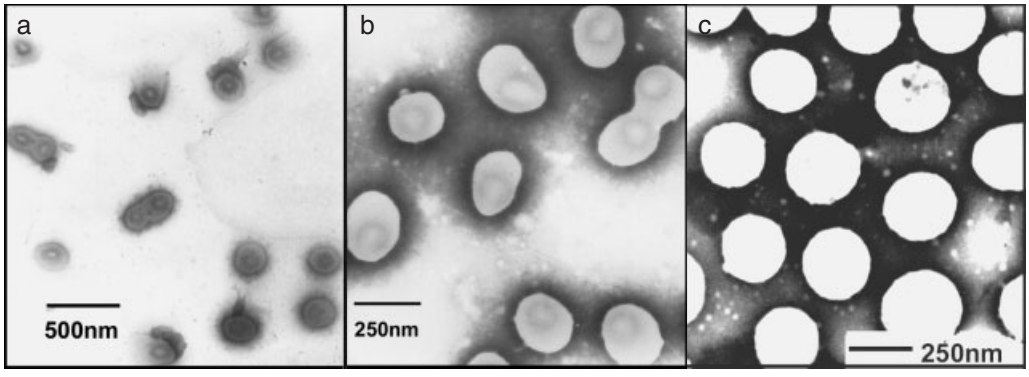

Figure 7. TEM images of a) N10-5 without staining, b) N10-5, negatively stained, and c) H10-5, negatively stained.

upon changing the temperature of the medium. Taking advantage of the on–off character around its LCST (about 32 °C), it is expected that the PNIPAM nanocages could be used for the protective encapsulation and controlled release of various biomacromolecules and drugs.

4. Experimental

Synthesis of N10-5 Spheres: First, initiator (AIBN, 5.63 mg, about 1.5 mol-% of the total monomer) was dissolved in a solution of PCL (8 mL, weight-average molecular weight, $M_w = 33\,000$, Scientific Polymer Product Inc.) in DMF (10 mg mL^{-1}). The solution was then added dropwise into stirred water (80 mL), while purging with nitrogen. Stirring was continued for 0.5 h, then NIPAM monomer (352 mg) and MBA crosslinker (48 mg, molar ratio to NIPAM 10 %) were added. The reaction was allowed to proceed for about 4 h at 76 °C. The PCL/PNIPAM particles were separated by centrifugation at an acceleration of about 270 000 g for 5 h. The hollow spheres were prepared by adding lipolase solution (8 vol.-%, Novozymes Co.) to the solution of the resultant particles, followed by gentle stirring for three days. The clean, hollow spheres were recovered by repeated dissolution–precipitation in cold–hot water.

FTIR spectra of the specimen films on aluminum foil, prepared from the solutions, were recorded on a Nicolet Magna 550 spectrometer. Malvern Autosizer 4700 and ALV/SP-125 Laser-light-scattering (LLS) spectrometers were used. The $\langle D_h \rangle$ and polydispersity index (PDI) were obtained by a cumulant analysis. The equilibrium time for each temperature was more than 30 min. SEM observations were performed using a Philips XL30 scanning electron microscope at an accelerating voltage of 20 kV. The samples were prepared by placing 5μL of the sphere solution on a glass substrate, and allowing them to dry freely. Gold sputtering was performed before the SEM observations. TEM observations were performed on a Philips CM 120 electron microscope at an acceleration voltage of 80 kV. The sample preparation for the TEM observations was similar to that for SEM, except that copper grids coated with thin films of Formvar and carbon were used as the substrate. Negative staining was performed by placing the sample grid on a drop of phosphate–tungstic acid solution (5 %) for about 10 min.

Received: August 19, 2004
Final version: September 21, 2004

[1] W. Meier, *Chem. Soc. Rev.* **2000**, *29*, 295.
[2] Y. Bae, S. Fukushima, A. Harada, K. Kataoka, *Angew. Chem. Int. Ed.* **2003**, *42*, 4640.
[3] D. T. Chiu, C. F. Wilson, A. Karlsson, A. Danielsson, *Chem. Phys.* **1999**, *247*, 133.
[4] F. Caruso, *Adv. Mater.* **2001**, *13*, 11.
[5] J. F. Ding, G. J. Liu, *Chem. Mater.* **1998**, *10*, 537.
[6] J. F. Ding, G. J. Liu, *J. Phys. Chem. B* **1998**, *102*, 6107.
[7] S. Steward, G. J. Liu, *Chem. Mater.* **1999**, *11*, 1048.
[8] H. Huang, E. E. Remsen, T. Kowalewski, K. L. Wooley, *J. Am. Chem. Soc.* **1999**, *121*, 3805.
[9] Q. Zhang, E. E. Remesen, K. L. Wooley, *J. Am. Chem. Soc.* **2000**, *122*, 3642.
[10] T. Sanji, Y. Nakatsuka, S. Ohnishi, H. Sakurai, *Macromolecules* **2000**, *33*, 8524.
[11] C. Nardin, T. Hirt, J. Leukel, W. Meier, *Langmuir* **2000**, *16*, 1035.
[12] F. Chécot, S. Lecommandoux, Y. Gnanou, H.-A. Klok, *Angew. Chem. Int. Ed.* **2002**, *41,* 1339.
[13] F. Chécot, S. Lecommandoux, H.-A. Klok, Y. Gnanou, *Eur. Phys. J. E* **2003**, *10*, 25.
[14] J. Z. Du, Y. M. Chen, *Macromolecules* **2004**, *37*, 5710.
[15] F. Caruso, H. Möhwald, *J. Am. Chem. Soc.* **1999**, *121*, 6039.
[16] C. Gao, E. Donath, H. Möhwald, C. Shen, *Angew. Chem. Int. Ed.* **2002**, *41*, 3789.
[17] C. Déjugnat, G. B. Sukhorukov, *Langmuir* **2004**, *20*, 7265.
[18] K. Glinel, G. B. Sukhorukov, H. Möhwald, V. Khrenov, K. Tauer, *Macromol. Chem. Phys.* **2003**, *204*, 1784.
[19] W. Meier, *Chimia* **1999**, *53*, 214.
[20] M. Sauer, D. Streich, W. Meier, *Adv. Mater.* **2001**, *13*, 1649.
[21] M. Okubo, Y. Konishi, H. Minami, *Colloid Polym. Sci.* **1998**, *276*, 638.
[22] O. Emmerich, N. Hugenberg, M. Schmidt, S. S. Sheiko, *Adv. Mater.* **1999**, *11*,1299.
[23] J. Jang, H. Ha, *Langmuir* **2002**, *18*, 5613.
[24] L. S. Zha, Y. Zhang, W. L. Yang, S. K. Fu, *Adv. Mater.* **2002**, *14*, 1090.
[25] J. V. M. Weaver, S. P. Armes, V. Butun, *Chem. Commun.* **2002**, 2122.
[26] L. Y. Chu, S. H. Park, T. Yamaguchi, *Langmuir* **2002**, *18*, 1856.
[27] J. X. Zhang, L. Y. Qiu, K. J. Zhu, Y. Jin, *Macromol. Rapid Commun.* **2004**, *25*, 1563.
[28] Q. G. Ma, E. E. Remsen, T. Kowalewski, J. Schaefer, K. L. Wooley, *Nano Lett.* **2001**, *1*, 651.
[29] H. J. Dou, M. Jiang, H. S. Peng, D. Y. Chen, *Angew. Chem. Int. Ed.* **2003**, *42*, 1516.
[30] J. Weaver, S. P. Armes, S. Liu, *Macromolecules* **2003***, 36,* 9994.
[31] J. F. Gohy, S. Antoun, R. Jérôme, *Macromolecules* **2001**, *34*, 7435.
[32] Y. Hu, X. Q. Jiang, Y. Ding, Q. Chen, C. Z. Yang, *Adv. Mater.* **2004**, *16*, 933.
[33] L. Y. Chu, T. Yamaguchi, S. Nakao, *Adv. Mater.* **2002**, *14*, 386.
[34] G. Ibarz, L. Dahne, E. Donath, H. Möhwald, *Adv. Mater.* **2001**, *13*, 1324.
[35] H. G. Schild, *Prog. Polym. Sci.* **1992**, *17,* 163.
[36] S. Fujishige, K. Kubota, I. Ando, *J. Phys. Chem.* **1989**, *93*, 3311.
[37] M. Wang, G. Z. Zhang, M. Jiang, D. Y. Cheng, *Macromolecules* **2001**, *34*, 7172.
[38] M. Wang, M. Jiang, F. L. Ning, D. Y. Cheng, *Macromolecules* **2002**, *35*, 5980.
[39] X. Y. Liu, M. Jiang, S. L. Yang, M. Q. Chen, *Angew. Chem. Int. Ed.* **2002**, *41*, 2950.
[40] Y. W. Zhang, M. Jiang, J. X. Zhao, J. Zhou, *Macromolecules* **2004**, *37*, 1537.
[41] D. H. Duan, D. Y. Cheng, M. Jiang, W. J. Gan, *J. Am. Chem. Soc.* **2001**, *123*, 12 097.
[42] M. Kuang, H. W. Duan, J. Wang, D. Y. Chen, *Chem. Commun.* **2003**, 496.
[43] G. Z. Zhang, A. Z. Niu, S. F. Peng, M. Jiang, Y. F. Tu, M. Li, C. Wu, *Acc. Chem. Res.* **2001**, *34*, 249.
[44] K. Chan, R. Pelton, J. Zhang, *Langmuir* **1999**, *15,* 4018
[45] A. Laukkanen, L. Valtola, F. Winnik, H. Tenhu, *Macromolecules* **2004**, *37,* 2268.
[46] Z. Gan, J. Fung, X. Jiang, C. Wu, W. K. Kuliche, *Polymer* **1999**, *40*, 1961.
[47] Z. Gan, T. Jim, M. Li, Z. Yuer, S. Wang, C. Wu, *Macromolecules* **1999**, *32*, 590.
[48] C. Wu, S. Q. Zhou, *Phys. Rev. Lett.* **1996**, *77*, 3053.
[49] W. Burchard, *Adv. Polym. Sci.* **1983**, *48*, 1.

5. Appendix

For a thick-wall hollow sphere with a radius of R and a wall thickness of $R/3$, if we assume that the density of the whole wall is homogeneous, then we have

$$< R_g^2 >= \frac{\int_{2R/3}^{R} 4\pi r^2 \cdot \rho \cdot r^2 dr}{\int_{2R/3}^{R} 4\pi r^2 \cdot \rho dr} = \frac{3r^5 \Big|_{2R/3}^{R}}{5r^3 \Big|_{2R/3}^{R}} = 0.74R^2 \quad (1)$$

$$< R_g > / < R_h >= \sqrt{< R_g^2 >} / < R_h >= \sqrt{0.74R^2}/R \approx 0.86 \quad (2)$$